Inverse methodology to determine mold set-point temperature in resin transfer molding process

Vincent Sobotka, Nicolas Lefevre, Yvon Jarny, Didier Delaunay

OPTIMAL SET-POINT TEMPERATURE IN RESIN TRANSFER MOLDING PROCESS

Vincent SOBOTKA, Nicolas LEFEVRE, Yvon JARNY, Didier DELAUNAY

Laboratoire de Thermocinétique de Nantes, UMR CNRS 6607, Ecole Polytechnique de l'Université de Nantes, La Chantrerie, Rue Christian Pauc, BP 50609 - 44306 Nantes, Cedex 03, France, Corresponding author's Email: vincent.sobotka@univ-nantes.fr

SUMMARY: This study consists of determining the optimal set point of the temperature of the fluid flowing through heat exchangers in a RTM mold so as to reach a predetermined thermal history in the composite part. The metallic mold is composed of several parts. Assembling these parts is not possible without introducing imperfect contacts that perturb heat transfer between them. Then in order to estimate the optimal set point of the temperature of the fluid, it is necessary in a first stage to evaluate the most influent thermal contact resistances between the parts. The determination of the TCR is achieved by an optimization approach and carried out on a 2D transverse cut of the mold. Experimental temperature measurements in the mold are matched to the computed responses of the heat conduction model. A least square criterion is minimized by using the conjugate gradient algorithm. The gradient of the criterion is determined by solving a set of adjoint equations. After the identification of these parameters, the same optimization method is used to compute the optimal set point of the fluid temperature. It is notable that the same set of adjoint equations is used to solve both problems.

KEYWORD: optimization, conjugate gradient algorithm, inverse method, RTM, metallic mold

1. Introduction

The use of structural pieces made of composite materials for aeronautic applications has increased a lot these last years. The Resin Transfer Molding is one of the processes used for the manufacture of such pieces. This process consists in injecting with low pressure a thermoset resin into a dry preform previously disposed into a closed mold. After the filling of the mold, the curing of the resin occurs. Then after the curing, the piece is removed from the mold and the next cycle begins. To keep this process profitable compared to other ones [1], the duration of the cycles must be reduced and the quality of pieces has to be controlled. Heat transfer appears to be a key point to satisfy these conditions in the different stages of the process.

In the case of aeronautic applications the molds are often metallic. The thermal control of these molds is achieved most of the time with the help of air oven or heated press. The use of air oven generates several constraints among which the financial investment is one of the most significant. Furthermore size of the manufactured pieces which become increasingly large may prevent the use of air oven. In these devices, the fluid which transfers heat to the piece is air and thermal inertia is so weak that even with high turbulent flow, the heat transfer remains weak and slow. As a consequence molding cycles are long and the accurate control of temperature is difficult.

For these reasons a prototype mold was designed to enable a better control of heat transfer in the piece [2] while increasing the rate of output. This mold possesses its own heat exchangers what makes it autonomous; the use of air oven becomes useless. The temperature of the fluid circulating in these exchangers can be controlled. Then from a desired cycle of temperature in the preform, the fluid temperature to impose at the heat exchangers inlet has to be determined. Moreover standard materials were chosen for the mold with the aim of reducing the manufacturing cost.

2. Experimental process

2.1. Description of the mold

The autonomous RTM mold is presented on Figure 1. The heating and the cooling of the piece is ensured by heat exchangers positioned on the external surface of the mold (Fig. 1). The fluid circulating in the exchangers is heated/cooled with temperature control units. PID controllers are used to regulate the temperature in the temperature control units so as to reach the desired set point temperature in the heat exchangers.

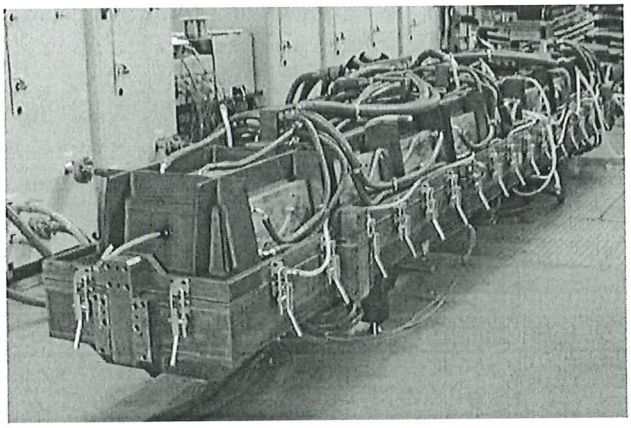

Fig.1. The autonomous RTM mold

The mold is composed of several metallic elements as indicated by the cut view in Fig.2.

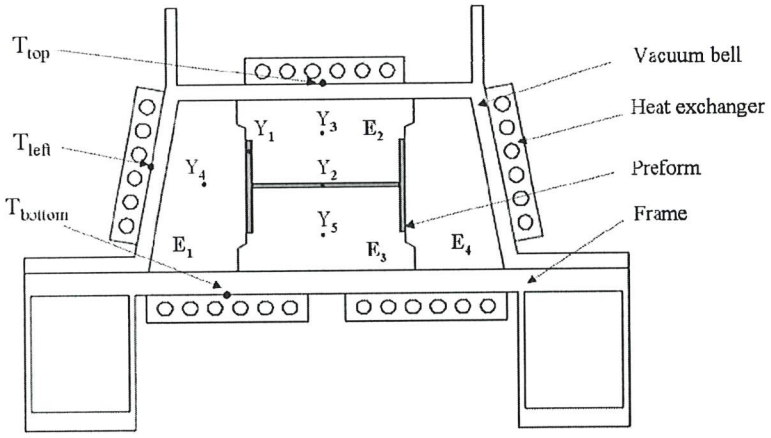

Fig. 2. 2D cut view of the instrumented mold.

The frame and the bell are made of steel. Four metallic elements (E_1,E_2,E_3,E_4) made of aluminum are positioned on the frame of the mold. The setting of these elements allows the

positioning of the preform. This assembly is then covered by the bell which is fixed on the frame.

The composite part manufactured with this mold is a beam which has a shape of H (Fig.3). It is composed of carbon reinforcement and epoxy resin. The piece length is about 9m and the thickness varies from 5mm to 9mm. Properties of the materials are given in Table 1.

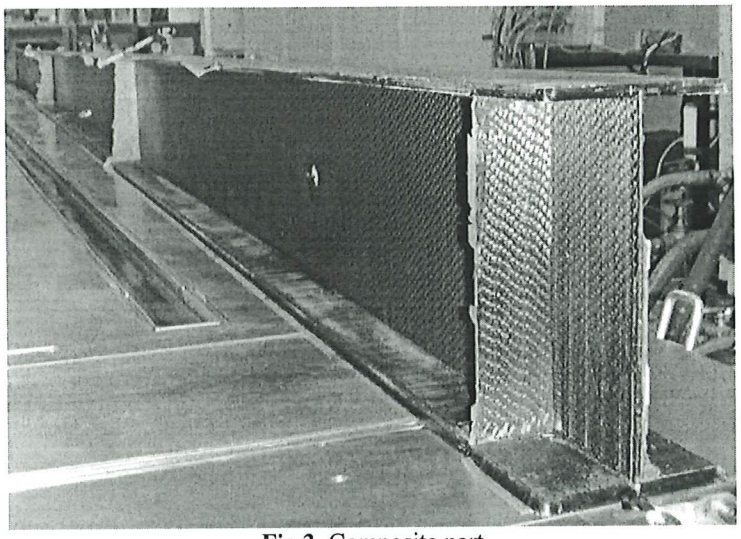

Fig.3. Composite part

Table 1 Properties of the materials

Material	**Aluminum**	**Steel**	**Carbon**	**Epoxy resin**	**Composite**
Zones	Heat exchangers E_1, E_2,E_3, E_4	Frame Vacuum bell	Preform	Preform	Part
Properties	ρ=2700kgm^{-3} Cp=900Jkg^{-1}K^{-1} λ=120Wm^{-1}K^{-1}	ρ=7800kgm^{-3} Cp=475Jkg^{-1}K^{-1} λ=30Wm^{-1}K^{-1}	ρ=1770kgm^{-3} Cp=1080Jkg^{-1}K^{-1} $\lambda_{\perp}$=0.22Wm^{-1}K^{-1} $\lambda_{//}$=3.00Wm^{-1}K^{-1}	ρ=1770kgm^{-3} Cp=1080Jkg^{-1}K^{-1} λ=0.1Wm^{-1}K^{-1}	τ_v=52% $\lambda_{\perp}$=0.6Wm^{-1}K^{-1} $\lambda_{//}$=3.6Wm^{-1}K^{-1}

2.2. Cycle parameters

Vacuum is applied in the part. The molding cycle consists in four steps:

#1. heating the carbon preform from ambient temperature to 120°C,
#2. injecting the resin in the perform at this temperature level,
#3. heating the part again to reach 180°C, so as to polymerize the resin,
#4. cooling the composite part down to ambient temperature before removing it from the mold.

A 2°C/min heating rate during the first step must be reached in the preform. It is then necessary to determine the set-point temperature of the fluid in the heat exchanger to reach such required cycle in the carbon preform. During such molding cycle, the temperature variations of the different elements of the mold evolve between 20°C and 180°C, As the elements are made of different materials, different thermal expansions occur and the contact between them does not remain constant according to temperature. Heat transfers being strongly dependant of these contacts, they must be quantified. Then Thermal Contact Resistances (TCR) are used to model the evolution of the contacts and their influence on the temperature field in the mold.

To point out the influence of TCR, two numerical resolutions of the conduction equation were performed by considering two different values of TCR (10^{-3}m²KW^{-1} in the first case and 5.10^{-}

$^{3}m^{2}KW^{-1}$ in the second case). The temperature difference computed in the carbon preform between these two cases reaches 5°C, for an increase of 35°C; a such 15% temperature variation cannot be neglected. Then determining the optimal set point is not possible without estimating in a first stage, the value of the most influent TCR between the different elements of the mold.

2.3. Instrumentation

The design of the thermal regulation allows considering 2D heat transfer in the transverse plane of the mold (Fig 2). Then the sensors used to record temperature are placed in a transverse section located in the middle of the length of the mold. Thermocouples of K-type are inserted at different locations in the carbon preform and in the mold. In the following, the readings of these sensors will be denoted by $(Y_i)_{i=1,5}$. As indicated in Fig. 2, Y_1 and Y_2 are located in the middle of the thickness of the preform; Y_3, Y_4 and Y_5 respectively in the elements E_2,E_1 and E_3 around the preform. Three additional thermocouples denoted by T_{left}, T_{bottom} and T_{top} on Figure 2, are placed under each heat exchanger, they give the temperature of the coolant fluid.

3. Numerical problem statement

3.1. Spatial domain

The goal of this work is to determine the temperature histories of the fluids so as to reach a predetermined cycle in the preform. However as explained in the previous section, this determination cannot be realized without having estimated in a first stage the TCR. There are thus two inverse heat conduction problems to solve. The first one consists in estimating the values of the different TCR (identification problem) and the second one in determining the optimal temperature set-points of the fluids in the heat-exchangers (control problem).
The numerical solutions of the heat conduction equation are computed over the spatial domain represented on Fig.4. It is simplified compared to the initial one (Fig.2). Indeed for reasons of symmetry, only half of the mold is represented. The frame of the mold is not represented either, the heat losses in this part are sufficiently weak to be neglected. Finally the heat exchangers are not modeled. Meshing the heat exchangers will increase the number of unknowns and will not improve significantly the results. Six different sub-domains are considered (Fig.4) and non perfect contact are assumed between each of them.
To estimate the TCR, temperature histories are imposed on the external surfaces Γ_3, Γ_4 and Γ_5 of the mold, thanks to the fluid of the exchangers, and they are used as boundary conditions. Experimentally these temperatures T_{left}, T_{bottom} and T_{top} are measured by the thermocouples placed under the heat exchangers. The recordings of the thermocouples $(Y_i)_{i=1,5}$ are used to identify the TCR. By solving the sensitivity problem according to the different TCR it is shown that the thermal contacts at the internal boundaries Γ_{11}, Γ_{12}, Γ_{15} and Γ_{17} have a very weak influence on the temperature field in the domain. For this reason, the TCR on these boundaries are fixed to a constant value of $5.10^{-3}Wm^{-1}K^{-1}$ and will not be estimated. Then only three significant TCR have to be determined: TCR_1, TCR_2 and TCR_3 and for convenient reasons, the estimated parameters are $h_i = (TCR_i^{-1})_{i=1,3}$, respectively on the boundaries Γ_{14},.Γ_{16} and Γ_{13}. They are evaluated as piecewise linear functions versus time.
In the control problem, the heat flux are estimated on boundaries $(\Gamma_i)_{i=1,2,3}$, in order to reach a prescribed 2°C/min heating rate in the carbon preform. Then the resulting temperatures on

these boundaries $(\Gamma_i)_{i=1,2,3}$ will determine the inlet fluid temperature inside the channels of the exchanger.

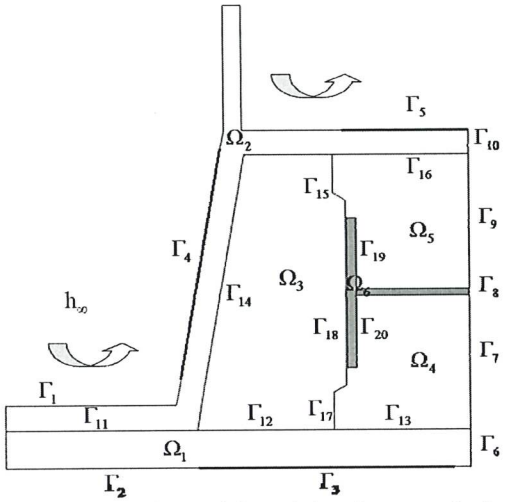

Fig. 4. 2D spatial domain used for solving the numerical problem.

3.2. The heat conduction model

For practical reasons only heat transfer equations of the sub-domain Ω_2 are presented (Eqn. 1). These equations can easily be generalized to the whole domain. In Eqn. (1) q(t) is a heat flux, h_∞ is the heat transfer coefficient with the surroundings, T_∞ is the ambient temperature and T_{left} and T_{top} are the temperatures measured by the thermocouples on boundaries Γ_4 and Γ_5. Thermophysical properties (ρ,Cp,λ) are specific to each sub-domain Ω_i. The model is used to predict the temperature field during the phases #1 (pre-heating), #3 (heating) and #4 (cooling). The injection phase #2 is not modeled. The presence of resin in the preform is taken into account by modifying its thermal properties as indicated in Table 1. A law of mixture is used to compute density and heat capacity. Thermal conductivities of the preform and of the composite part were measured by Lecointe [3]. Moreover the mold has such an important thermal inertia that the heat released during polymerization can be neglected in the energy balance equations.

$$
\begin{aligned}
&\rho Cp\frac{\partial T_{\Omega_2}}{\partial t} = \nabla.\left(\lambda \nabla T_{\Omega_2}\right) && in\ \Omega_2, t>0 \\
&-\lambda\frac{\partial T_{\Omega_2}}{\partial n}\bigg|_{\Gamma_{16}} = h_2\left(T_{\Omega_5} - T_{\Omega_2}\right) && on\ \Gamma_{16}, t>0 \\
&-\lambda\frac{\partial T_{\Omega_2}}{\partial n}\bigg|_{\Gamma_{10}} = 0 && on\ \Gamma_{10}, t>0 \\
&T_{\Omega_2} = T_0 && in\ \Omega_2, t=0 \\
&-\lambda\frac{\partial T_{\Omega_2}}{\partial n}\bigg|_{\Gamma_{14}} = h_1\left(T_{\Omega_3} - T_{\Omega_2}\right) && on\ \Gamma_{14}, t>0 \\
&-\lambda\frac{\partial T_{\Omega_2}}{\partial n}\bigg|_{\Gamma_1} = h_\infty\left(T_\infty - T_{\Omega_2}\right) && on\ \Gamma_1, t>0 \\
&-\lambda\frac{\partial T_{\Omega_2}}{\partial n}\bigg|_{\Gamma_4\cup\Gamma_5} = q(t) && \\
&\text{or}\ \begin{cases} T_{\Omega_2}\big|_{\Gamma_4} = T_{left}(t) \\ T_{\Omega_2}\big|_{\Gamma_5} = T_{top}(t) \end{cases} && on\ \Gamma_4\cup\Gamma_5, t>0
\end{aligned}
\qquad (1)
$$

Both inverse problems are formulated in the least-square sense and consist in determining the optimal solution which minimizes the functional:

$$J(\beta)=\sum_j \int_0^{t_f} \left\| Y_j(t)-T(x_j,y_j,t;\beta) \right\|^2 dt \tag{2}$$

Where β corresponds to the parameters which have to be determined and T is the solution of heat equation (1) on the whole domain. The unknowns to be determined are:

- $\beta=(h_i)_{i=1,3}$ for the identification problem, and T_{left}, T_{top} and T_{bottom} are imposed.
- $\beta=q(t)$ on $\Gamma_3 \cup \Gamma_4 \cup \Gamma_5$ for the input problem, and $(h_i)_{i=1,3}$ are known.

3.3. Conjugate Gradient Algorithm (CGA)

These two problems are solved by using the classical CGA. This algorithm is iterative and consists at each iteration k+1, in correcting the previous estimate β^k according to $\beta^{k+1}=\beta^k+\rho^k w^k$ in order to obtain $J(\beta^{k+1})<J(\beta^k)$. In this expression w^k is the search direction and ρ^k the descent length. By naming ∇J the vector gradient of the functional J, the vector w^k and the scalar ρ^k are determined according to the gradient equations:

$$w^k=-\nabla J^k+\gamma^k w'^{k-1} \tag{3}$$

$$\gamma^k=\frac{\left\|\nabla J^k\right\|}{\left\|\nabla J^{k-1}\right\|} \text{ with } \gamma^0=0 \tag{4}$$

The length of descent ρ is computed to minimize the following scalar function $\phi(r)$ either by solving the sensitivity problem or by using a minimization algorithm [4]:

$$\phi(r)=\sum_j \int_0^{t_f} \left\| Y_j(t)-T(x_j,y_j,t;\beta^k+rw^k) \right\|^2 dt \tag{5}$$

3.4. The Adjoint Problem

Let us introduce the Lagrange multiplier ψ [5,6] and the Lagrangian $L(\psi,T,\beta)$ associated to the optimization problem defined by (2) and the constraint corresponding to the first equation of the system (1):

$$L(\psi,T,\beta)=\int_{t=0}^{t_f}\left\{\left(\sum_j \left\|Y_j-T_j\right\|^2\right)-\left\langle \psi,\rho Cp\frac{\partial T}{\partial t}-\nabla.(\lambda\nabla T)\right\rangle_{(\Omega_i)_{i=1,6}}\right\}dt \tag{6}$$

When the adjoint variable is fixed the differential of L is equal to

$$\delta L=\frac{\partial L}{\partial T}\delta T+\frac{\partial L}{\partial \beta}\delta\beta \tag{7}$$

The Lagrange multiplier is then chosen in order to verify:

$$\frac{\partial L}{\partial T}\delta T = 0, \forall \delta T \tag{8}$$

This condition leads to find the Lagrange multiplier so as to be the solution of the following set of adjoint equations [7]. As for the direct problem, only the adjoint equations concerning the sub-domain Ω_2 are presented.

$$\begin{array}{ll|ll}
\rho Cp\dfrac{\partial \psi_{\Omega_2}}{\partial t} + \nabla.\left(\lambda \nabla \psi_{\Omega_2}\right) = & & -\lambda\dfrac{\partial \psi_{\Omega_2}}{\partial n}\Big|_{\Gamma_{14}} = h_3\left(\psi_{\Omega_3} - \psi_{\Omega_2}\right) & on\ \Gamma_{14}, t>0 \\
\sum_j (Y_j - T)\delta(x - x_j)\delta(y - y_j) & in\ \Omega_2, t>0 & & \\
-\lambda\dfrac{\partial \psi_{\Omega_2}}{\partial n}\Big|_{\Gamma_{16}} = h_5\left(\psi_{\Omega_5} - \psi_{\Omega_2}\right) & on\ \Gamma_{16}, t>0 & -\lambda\dfrac{\partial \psi_{\Omega_2}}{\partial n}\Big|_{\Gamma_1} + h_\infty T_{\Omega_2} = 0 & on\ \Gamma_1, t>0 \\
-\lambda\dfrac{\partial \psi_{\Omega_2}}{\partial n}\Big|_{\Gamma_{10}} = 0 & on\ \Gamma_{10}, t>0 & -\lambda\dfrac{\partial T_{\Omega_2}}{\partial n}\Big|_{\Gamma_4 \cup \Gamma_5} = 0 \text{ or } \psi_{\Omega_2}\Big|_{\Gamma_4 \cup \Gamma_5} = 0 & on\ \Gamma_4 \cup \Gamma_5, t>0 \\
\psi_{\Omega_2} = 0 & in\ \Omega_2, t = t_f & &
\end{array} \tag{9}$$

When the adjoint variable is determined from the set of equations (9), the differential of L is equal to $\delta L = \dfrac{\partial L}{\partial \beta}\delta\beta$. Furthermore, when T verifies equations (1) of the direct problem, we get $\delta L = \delta J$. Note that the adjoint problem remains the same for the two problems considered.

3.5. The Components of Gradient

- Identification problem: $\beta = (h_i)_{i=1,3}$.

The coefficient h_i is evaluated as a function of time. It is then approximated in the form $h_i(t) = \sum_{k=1}^{N_p} h_{ik}\sigma_k(t)$, where σ_k is a given set of N_p basis functions over the time interval. The gradient components are then equal to:

$$\frac{\partial J}{\partial h_{ik}} = \int_{t=0}^{t_f}\int_{\Gamma_{h_i}} (\psi_m - \psi_n)(T_n - T_m)\sigma_k d\Gamma dt \quad for\ i=1,3 \tag{10}$$

where Γ_{h_i} corresponds to the boundary on which the parameter h_i is applied. ψ_m and ψ_n represent the adjoint fields on the domains Ω_m and Ω_n delimited by the boundary Γ_{h_i}. This vector possesses $3 \times N_p$ components.

- Input problem: $\beta = (q_i)_{i=1,N_q}$

The heat flux q(t) is approximated in the form $q(t) = \sum_{k=1}^{N_q} q_k\sigma_k(t)$ where σ_k is a given set of N_q basis functions over the time interval. The gradient components are then equal to:

$$\frac{\partial J}{\partial q_k} = \int_{t=0}^{t_f} \int_{\Gamma_3 \cup \Gamma_4 \cup \Gamma_5} \psi_i \sigma_k d\Gamma dt \tag{11}$$

A general algorithm of these two problems is presented on Figure 5.

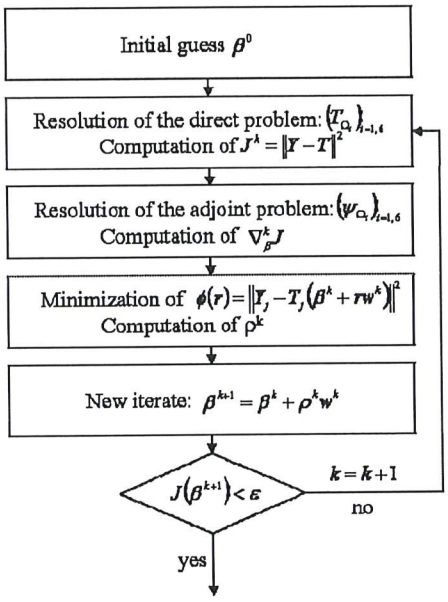

Fig. 5. General algorithm

4. Results and discussion

In the following, numerical results coming from the resolution of both inverse problems are presented, as well as the comparison with experimental molding results.

4.1. Estimation of Thermal Contact Resistances

The input data used to solve the estimation problem come from an experimental molding. Fig. 6 represents the temperatures given by T_{bottom}, T_{left}, T_{top}. The temperatures of these three thermocouples are very close indicating that the same set-point is used in each heat exchanger. These temperatures are used as boundary conditions in this problem. Fig.7 represents the temperatures given by thermocouples $(Y_i)_{i=1,5}$ during the same molding.

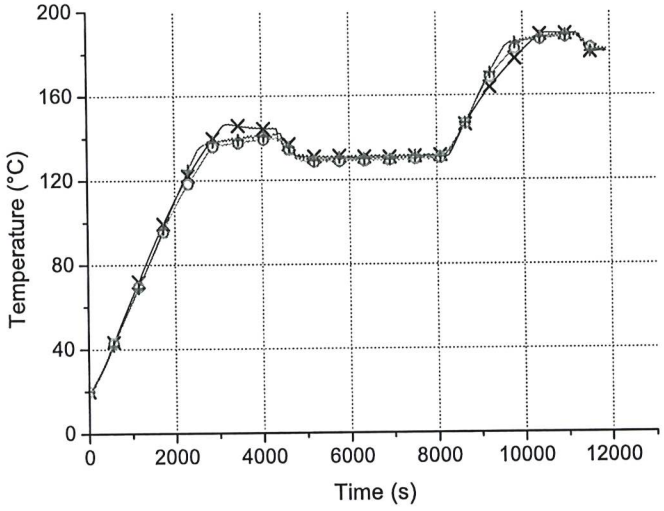

Fig. 6. Temperatures at the surface of the mold (× T_{bottom}, O T_{left}, + T_{top}).

Temperatures recorded by $(Y_i)_{i=1,5}$ evolve between 20°C and 180°C. The cycle can be divided into two main steps. The first one corresponds to the rise between ambient temperature and the first plateau at 120°C. During this phase #1, the temperature of Y_4 (thermocouple located in the left element E_1) is much higher than the other ones. This evolution indicates that heat transfer is much more important between the bell and the element E_1 than between the bell and the other elements. The evolutions given by Y_1 and Y_2 indicate that temperature is higher in the preform than in the elements E_2 and E_3. Heat is then mainly transferred through the element E_1.

Injection (phase #2) occurs between 7000s and 8000s. After the end of injection the second rise occurs between 122°C and 180°C. During this phase #3, the gap between the temperatures and especially with the thermocouple Y_4 are smaller. Two phenomena explained this evolution. The increase of temperature causes an expansion of the elements of the mold. Thermal expansion of aluminum being higher than steel, contacts between the elements $(E_i)_{i=1,4}$ and the bell are improved. Therefore contact becomes better while increasing temperature. Besides the design of the mold ensures a good contact between the elements at the maximum temperature i.e. at 180°C. Since resin is injected at 120°C there are at this temperature interstices between the elements of the mold. During the injection the resin flows in these interstices, improving the contact between the elements of the mold and thus improving heat transfer.

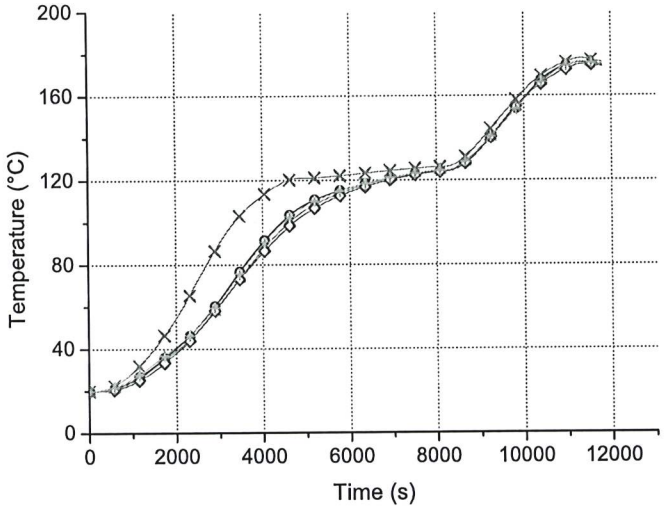

Fig.7. Temperature recorded by $(Y_i)_{i=1,5}$ (O Y_1, Δ Y_2, ◇ Y_3, × Y_4, + Y_5)

Fig. 8 represents the evolution of the norm of the LS-criterion J during the estimation of the TCR. In this problem 9 values are estimated for each TCR. About 70 iterations are necessary to reach the solution with an initial guess of 100W/m².K for each $(h_i)_{i=1,3}$.

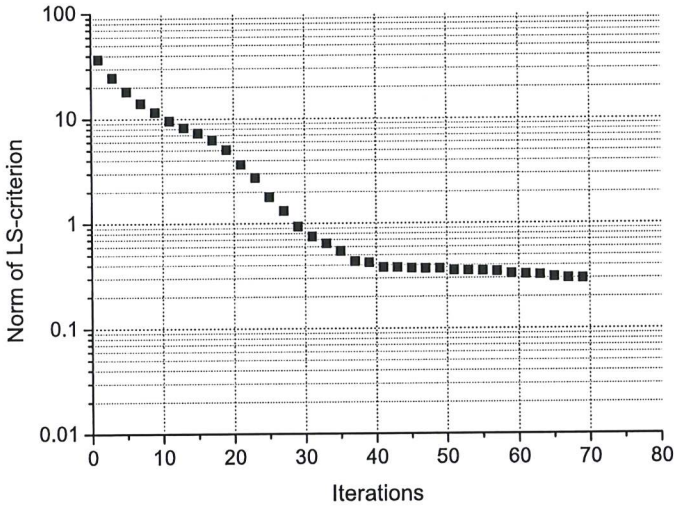

Fig. 8. Norm of the LS-criterion – Identification of TCR

The results of this estimation are represented by Fig.9. TCR are estimated as functions of time. The values of TCR_1, TCR_2 and TCR_3 are then correlated respectively to the temperature of the elements E_1, E_2 and E_3. The evolution of TCR can be divided into two stages: before and after injection. Before injection values of TCR decrease according to temperature. This evolution due to thermal expansion is in compliance with the preceding explanations. The value of TCR1 is smaller than the two others. This evolution is logical, the contact on this boundary being better than the others. The evolution of the values of the resistances determined by the code is thus coherent with the observations carried out previously.

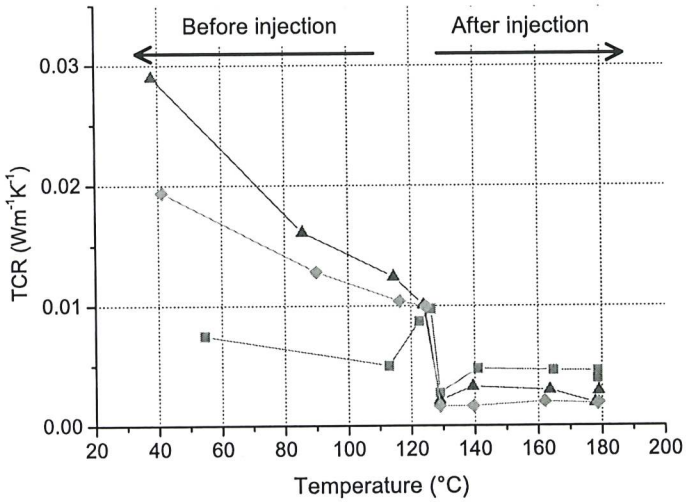

Fig. 9. Estimated TCR (TCR1 ■, TCR2 ▲, TCR3 ♦)

4.2. .Determination of the Optimal Temperature Set-Points

Once the TCR are estimated, one can determine the optimal heat flux on boundaries $(\Gamma_i)_{i=3,4,5}$ to reach a desired temperature history in the preform. The design of the mold allows considering that the desired temperature in the preform can be reached by applying the same heat flux in each heat exchanger. However this method also permits to estimate different heat fluxes in each heat exchanger. The heat flux is searched as a linear piecewise function defined by $q(t)=\sum_{k=1}^{N_q} q_k \sigma_k(t)$ with N_q=70 which means that 70 unknowns have to be estimated over the time interval [0s; 3.10^4s]. The desired temperature is represented on Fig.10. This profile is used as the target to reach (Y) in the functional J. Only points inside the domain representing the preform (Ω_6) can be used in this estimation. We choose to use two points placed in the location of Y_1 and Y_2. Note that no experiment is necessary to carry out this estimation. Fig. 10 represents the desired and estimated temperature in the preform in the location of Y_1 and Y_2. The really good agreement obtained between the two sets of temperatures during the whole cycle proves that the inverse method manages to estimate correctly the heat flux.

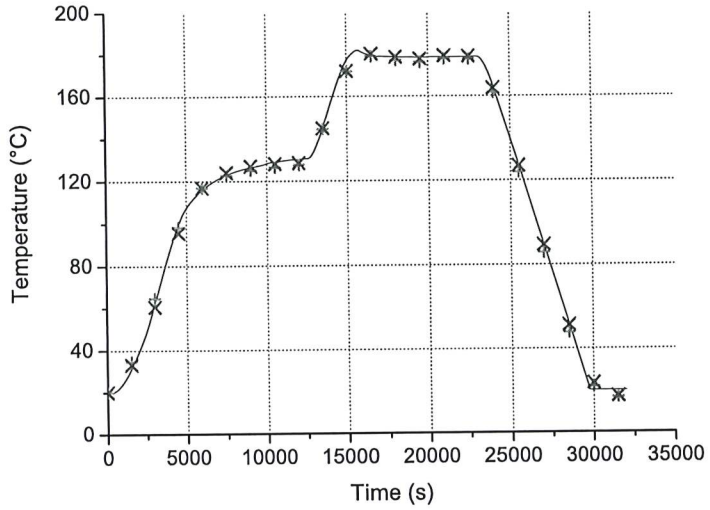

Fig. 10. Desired (—) and estimated temperatures (+ Y_1, × Y_2)

Fig.11 represents the heat flux determined by the algorithm to reach the predetermined temperature. This evolution can be divided into three parts. The first one corresponds to the first rise of heating and the first plateau at 120°C (between 0s and 12000). During this stage the heat flux increases rapidly to attain 10000W/m² at about 2500s. It decreases then linearly to reach a value which remains quasi constant between 6000s and 12000s. This evolution permits the temperature of the preform to increase linearly at the right rate. The decrease of the heat flux from 2500s prevents the temperature of the preform to heat over the desired temperature of the first plateau. The heat flux anticipates therefore the evolution of the temperature so as to vanquish the thermal inertia of the mold and of the preform. The same kind of evolution occurs during the second heating ramp and then during the cooling. In particular the heat flux remains constant and positive during the two plateaus at 120°C and 180°C to compensate the heat losses by convection with the surroundings. At the end of the cooling the heat flux equals zero indicating an isothermal state at ambient temperature. The composite part can then be removed from the mold.

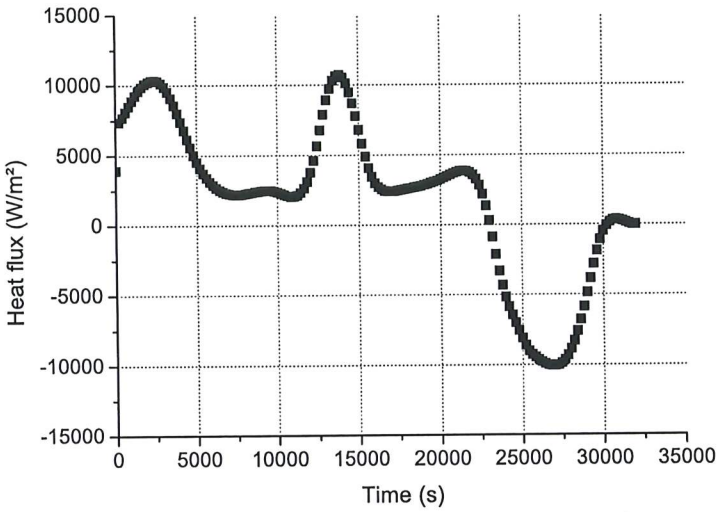

Fig. 11. Optimal heat flux.

From the estimated heat flux it is possible to compute the temperature of the fluid in the heat exchangers by using the same kind of inverse method. It is then possible to check the results of the method by carrying out a molding in which the estimated set-point temperature is imposed in the heat exchangers and by comparing the experimental temperatures of the preform given by Y_1 and Y_2 with the desired temperature imposed during the computation. However this molding has not been carried out yet. The temperatures of Y_1 and Y_2 resulting from a molding were chosen as the desired temperature and we determined the temperature to impose in the heat exchanger to reach this profile. We compared then the temperature estimated by the algorithm with the experimental one. This result is presented on Fig.12. This figure shows a good agreement between the determined and the measured temperature. This profile of temperature is not intuitive notably the over heating before each isothermal step. This type of method can be very efficient to reach the optimal set-point of temperature.

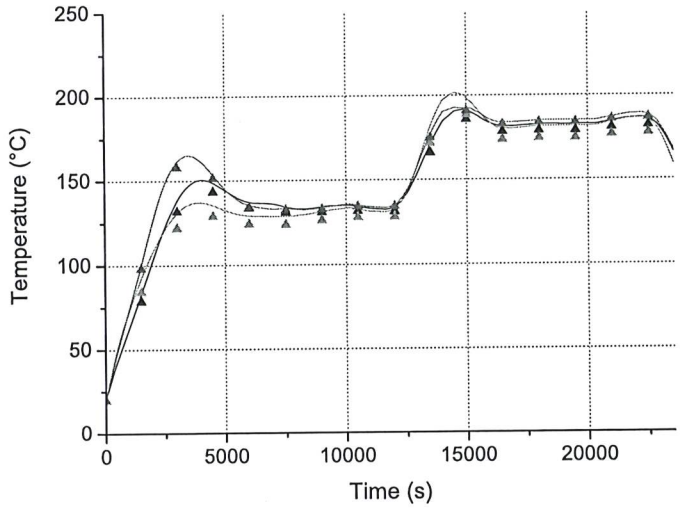

Fig. 12. Estimated (+) and experimental (—) temperatures in heat exchanger.

5. Conclusion

An RTM autonomous metallic mold was developed for aeronautic applications. This mold is equipped with heat exchangers which prevents the use of air oven. This approach presents several advantages, among which one can note: less investment, possibility to manufacture large sized parts, better control of temperature history than in an air oven.
The conjugate gradient algorithm was used to evaluate the most significant thermal contact resistances between the different parts of the mold. A decrease of these resistances according to temperature was pointed out. This decrease is due to the thermal expansion of the metallic elements of the mold and to the presence of resin after the injection.
Then the optimal heat flux that allows reaching a predetermined cycle of temperature into the preform was estimated. The set-point temperature in the fluid circulating in the heat exchangers was computed from this heat flux. The set-point is not intuitive. The results show a very good agreement between the computed and desired temperatures.

Acknowledgement

This work has taken place in the framework of the "RTM Région" consortium. The authors would like to thank the French Region Pays de la Loire and the European Union for its financial support as well as the "Pôle de Compétitivité EMC2", and our partners (especially Airbus, CDPlast and CERO) for their collaboration. Special thanks to F.Beaudrap for the management of the program.

References

1. J.Verrey, M.D.Wakeman, V.Michaud, and J.-A.E.Manson. Manufacturing cost comparison of thermoplastic and thermoset RTM for an automotive floor pan. Composites Part A 2006, 37(1):9-22

2. V.Sobotka and D.Delaunay. Analysis and Control of Heat Transfer in an Industrial Composite Mold in RTM Polyester Automotive Process, J. of Reinf. Plast and Comp.2007, 26(9): 881-901

3. D.Lecointe. Caractérisation et simulation des processus de transferts lors d'injection de résine pour le procédé RTM, PhD Thesis, Université de Nantes, 1999

4. R.P.Brent, Algorithms for Minimization Without Derivatives, Prentice-Hall, 1973, Dover, 2002

5. Y.Jarny, The Adjoint Method to Compute the Numerical Solutions of Inverse Problems, Inverse Engineering Handbook, Woodbury K.A. editor, CRC Press LLC,.ISBN: 0-8493-0861-5, (2003).

6. J.-L.Bailleul, V.Sobotka, D.Delaunay. and Y.Jarny, Inverse Algorithm for Optimal Processing of Composite Materials, Composites: Part A 2003,34(8): 695-708

7. R.Abou khachfe and Y.Jarny, Determination of Heat sources and Heat Transfer Coefficient for Two-Dimensional Heat Flow – Numerical and Experimental Study, Int. J. of Heat and Mass Transfer 2001, 44(7): 1309-1322